ACSNANO
www.acsnano.org
ARTICLE

Photoprompted Hot Electrons from Bulk Cross-Linked Graphene Materials and Their Efficient Catalysis for Atmospheric Ammonia Synthesis

Yanhong Lu,[†,§,∥] Yang Yang,[†,‡,∥] Tengfei Zhang,[†,‡,∥] Zhen Ge,[†,‡] Huicong Chang,[†,‡] Peishuang Xiao,[†,‡] Yuanyuan Xie,[⊥] Lei Hua,[⊥] Qingyun Li,[⊥] Haiyang Li,[⊥] Bo Ma,[‡] Naijia Guan,[‡] Yanfeng Ma,[†,‡] and Yongsheng Chen*[,†,‡]

[†]The Centre of Nanoscale Science and Technology and Key Laboratory of Functional Polymer Materials, State Key Laboratory and Institute of Elemento-Organic Chemistry, Collaborative Innovation Center of Chemical Science and Engineering (Tianjin), College of Chemistry and [‡]School of Materials Science and Engineering, The National Institute for Advanced Materials, Nankai University, Tianjin 300071, China

[§]School of Chemistry & Material Science, Langfang Teachers University, Langfang 065000, China

[⊥]Key Laboratory of Separation Science for Analytical Chemistry, Dalian Institute of Chemical Physics, Chinese Academy of Sciences, Dalian 116023, China

Supporting Information

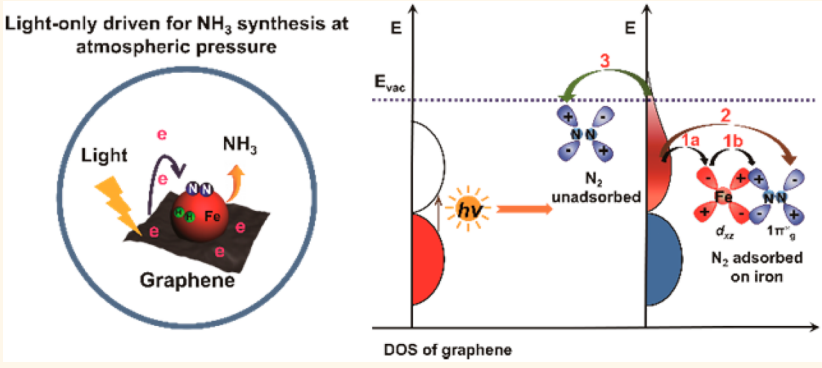

ABSTRACT: **Ammonia synthesis is the single most important chemical process in industry and has used the successful heterogeneous Haber−Bosch catalyst for over 100 years and requires processing under both high temperature (300−500 °C) and pressure (200−300 atm); thus, it has huge energy costs accounting for about 1−3% of human's energy consumption. Therefore, there has been a long and vigorous exploration to find a milder alternative process. Here, we demonstrate that by using an iron- and graphene-based catalyst, Fe@3DGraphene, hot (ejected) electrons from this composite catalyst induced by visible light in a wide range of wavelength up to red could efficiently facilitate the activation of N_2 and generate ammonia with H_2 directly at ambient pressure using light (including simulated sun light) illumination directly. No external voltage or electrochemical or any other agent is needed. The production rate increases with increasing light frequency under the same power and with increasing power under the same frequency. The mechanism is confirmed by the detection of the intermediate N_2H_4 and also with a measured apparent activation energy only ~1/4 of the iron based Haber−Bosch catalyst. Combined with the morphology control using alumina as the structural promoter, the catalyst retains its activity in a 50 h test.**

KEYWORDS: *graphene, photoprompted, hot electron, ammonia synthesis, atmospheric pressure*

Ammonia synthesis is profoundly important for both human beings and the earth's ecosystem. This is partially reflected in the fact that the scale of both industry[1] and biological fixation for its production[2] is at ~200 ×

Received: September 25, 2016
Accepted: November 7, 2016
Published: November 7, 2016

DOI: 10.1021/acsnano.6b06472
ACS Nano 2016, 10, 10507−10515

10^6 tons each year,[3] which is the foundation sustaining the life on the planet. With this tremendous scale and implication, it is striking to note that these two processes follow two very different mechanisms under extremely different conditions. The natural one proceeds with very high efficiency under ambient conditions, while the industrial one has always been carried out under both high, harsh temperature and pressure (300−500 °C and 200−300 atm).[3,4] The large scale of the industry synthesis comes at a huge price as it has been the single most energy-consuming industrial chemical process in the world, currently consuming approximately 1−3% of the entire world energy's consumption. The remarkable difference between these two processes is due to their different catalyst systems. The first one uses the natural nitrogenase enzyme, and the industrial one, *e.g.*, the Haber−Bosch process, known as the "bellwether reaction in heterogeneous catalysis", uses the iron based Haber−Bosch catalyst (HB catalyst),[1,5] which consists of primarily reduced magnetite ore (Fe_3O_4). Despite its high pressure and temperature requirement and with a thermodynamically limited conversion, after almost a century the HB process still remains the dominant route for ammonia synthesis, partially due to its highly efficient energy consumption. As a result, it has been a long-standing and "Holy Grail" objective of significant and international studies to find an alternative to the energy-consuming Haber−Bosch process to produce this fundamental chemical.[6]

During the last century, tremendous studies and many pioneering works have been carried out in the pursuit for a milder method, including two main strategies of (a) mimicking the nature nitrogenase enzyme[4,7] and (b) designing a milder catalyst system based on currently the most successful HB catalyst,[8] including Ru-based catalyst.[9,10]

Other proposed approaches for milder conditions include using electrochemical[11−15] systems based on semiconductors or proton conductors,[11,16] prompted by certain light wavelengths and/or at the expense of scarifying agents.[13,17,18] Recently, an efficient electrochemical process with a rate of 2.4×10^{-9} mol s^{-1} cm^{-2} operated at 200 °C by the electrolysis of air and steam in molten sodium hydroxide with nano-Fe_2O_3 as the catalyst was reported by Licht et al.[19] An approach was also recently reported by Hosono's group, where the activity of the Ru catalyst, operated at ∼400 °C, was significantly enhanced using a stable electride as the electron promoter.[20] Hamers et al., using a H-terminated diamond as a solid electron source under light illumination, also reported an electrochemical ammonia synthesis by solvated electrons in water.[21] Very recently, an approach was reported where cadmium sulfide nanocrystals can be used to photosensitize the nitrogenase molybdenum−iron protein with visible light illumination.[22] Overall, such an ideal process, if possible, might be to use clean and unlimited (sun) light as the energy and start with elemental nitrogen directly as occurs in the nature. Unfortunately, while tremendous work and effort have been carried out for over a century, no economically viable alternative has been put into practice so far.

The main reason for this unsuccessful but long journey, followed by so many scientists, is mainly due to the special and very inert molecular structure of the nitrogen molecule, which has an extremely high bond energy (945 kJ mol^{-1}) and the absence of the permanent dipole of the triple bond in the nitrogen molecule.[23] Importantly, it should be also noted that while tremendous work has been done, there are still many puzzles for the mechanisms of both the natural[7,24,25] and industry[1,3,5] synthesis of ammonia.

Recently, it has been found that graphene can achieve a reverse saturation state with a high density (∼10^{13} cm^{-2})[26] of hot electrons well above the Fermi level with even visible light, and these hot electrons can even be ejected out following an Auger-like light-induced electron emission (LIEE) mechanism[27,28] due to its Dirac band structure, which causes the conventional relaxation of the excited electrons to be bottlenecked.[29−31]

With these in mind, we intend to test the idea of using these light-generated highly energetic hot/free electrons as a most powerful and clean reducing agent for some of the most difficult and landmark reactions or reactions that are otherwise unachievable using conventional methods or with harsh conditions. These could include reactions such as ammonia synthesis from molecular nitrogen directly at mild conditions. Indeed, when such a graphene-based iron catalyst is used, a light-driven and efficient ammonia synthesis from its elements directly at ambient pressure was achieved where graphene worked as an electron reservoir following the LIEE mechanism under even visible light illumination and the generated hot/free electrons efficiently prompted the activation of nitrogen and hydrogen and thus ammonia synthesis.

RESULTS AND DISCUSSION

Catalytic Activity. The catalyst Fe@3DGraphene (Fe@3DG), denoted for iron oxide loaded on the bulk three-dimensional cross-linked graphene (3DG) material developed recently,[27] was obtained using common iron precursors and graphene oxide through a simple and easily scalable solvothermal reaction followed by an annealing process, as detailed in the Supporting Information. The material has a conductivity of ∼0.23 S m^{-1} and a density of ∼0.7 mg cm^{-3}. As has been demonstrated before,[27,28] the 3DG material has a very unique structure and morphology, similar to that of a monolithic polymer but with graphene sheets as the monomer which cross-links together mainly at the edge. This makes such a material retain the nature of individual graphene sheets and thus exhibit essentially all of the remarkable properties of individual graphene sheets but at a bulk state, including its remarkable mechanical and (opto)electronic properties.[27,28] The structure and morphology analyses of Fe@3DG are illustrated in the Supporting Information (Figures S1−S5). Overall, the structure and morphology of this catalyst barely change from the template of 3DG, where iron oxide is distributed homogeneously throughout at the nanoscale on the surface of graphene sheets. It is well understood that the nanoscale nature of iron domain is critical for its catalytic activity of iron-based catalysts.[1,9,19] Thus, the size of iron oxide loaded on 3DG was controlled at such a scale, achieved by using a simple wet chemistry approach. The catalytic activity was measured using a homemade fixed-bed continuous-flow reactor containing Fe@3DG catalyst, where the mixture of H_2/N_2 (3/1, v/v) was flowed through the reactor with a Hg lamp (or others) continuum light inside and water cooling outside (Figure S7). Note that even with vigorous external cooling the stable temperature of the actual catalytic reaction inside the reactor could only be controlled and measured at ∼200 °C due to the light heating. The catalyst activation (from catalyst precursor iron oxide to α-Fe) should be achieved at the initial period in the reduction environment as that for the HB catalyst.[3] The confirmation of product ammonia (Figure S8) and its real-time monitoring were performed using a recently developed, highly sensitive online charge-transfer ionization

DOI: 10.1021/acsnano.6b06472
ACS Nano 2016, 10, 10507−10515

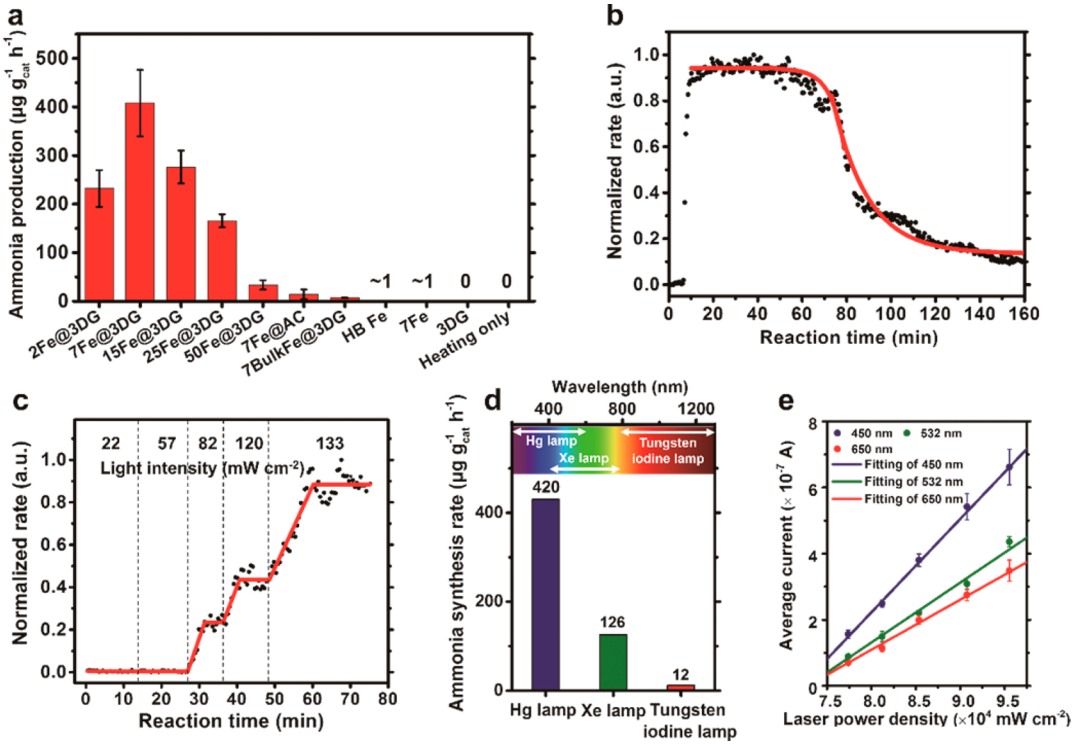

Figure 1. Catalytic performance of Fe@3DG at atmospheric pressure. (a) Amount of ammonia produced per gram catalyst per hour under Hg lamp illumination and "heating only" with external heating to the same temperature (but no light) using the same 7Fe@3DG. (b) Real-time normalized ammonia synthesis rate using catalyst 7Fe@3DG. (c) Relationship of ammonia synthesis rate *vs* light intensity. (d) Wavelength dependence of ammonia synthesis rate using 500 W Hg, Xe, and tungsten iodine lamps, respectively, under the same conditions. (e) Electron emission (current) dependence on laser wavelength and power density. Reaction conditions: synthesis gas, H_2/N_2 = 3 (v/v) with a flow rate of 20 mL min^{-1}; pressure, 1 atm; 500 W high-pressure Hg lamp used as the light source unless otherwise indicated.

time-of-flight mass spectrometry (CTI-TOFMS).[32] The ammonia amount was also quantitatively measured using an indophenol blue method.[21] The catalysts were studied with varied iron loadings, support materials, and preparation methods as detailed in the Experimental Section and the Supporting Information.

To better understand the mechanism of this mild ammonia synthesis, a series of catalysts with different loadings of Fe (2Fe@3DG, 7Fe@3DG, 15Fe@3DG, 25Fe@3DG, and 50Fe@3DG) and various control experiments/catalysts have been investigated under the same conditions (see more details below). The control reactions included that using the same Fe precursor on activated carbon (7Fe@AC), bulk Fe on 3DG, the HB catalyst, and blank experiments with only nano Fe or 3DG or without light. As can be seen in Figure 1a, the catalysts tested with different loadings of iron all showed significantly higher activity than those of the reference catalysts as discussed below, and the best activity was achieved for 7 wt % Fe loading (7Fe@3DG) with a space−time yield at 408 ± 68 μg g_{cat}^{-1} h^{-1} measured using the indophenol blue method,[21] which is among the highest reported for ammonia synthesis with milder methods reported recently (Table S2). When 7Fe@AC (the same iron loading but on activated carbon, Figures S1 and S6) was sued, less than 1 order smaller amount of ammonia production was observed. Furthermore, 7BulkFe@3DG (bulk size of iron oxide loaded on the same 3DG) demonstrated a much smaller catalytic activity compared with 7Fe@3DG, indicating that the size of iron plays a significant role as widely observed in the literature.[19] Other control reactions were also carried out under the same conditions, including that using the landmark fused iron HB catalyst (HB Fe), 7Fe (same iron catalyst as that loaded on 7Fe@3DG, but not on the 3DG template, Figures S1 and S6), and 3DG only, all gave no detectable or negligible amount of ammonia as shown in Figure 1a. Most notably, the control reaction using the same catalyst 7Fe@3DG under the same conditions (including temperature) but without light (Figure S9) generated only a negligible amount of ammonia. A typical plot of real-time ammonia synthesis rate *vs* time over 7Fe@3DG is shown in Figure 1b, where after the initial activation the activity retains steady for the first ~60 min. The drop of activity of the catalysts after a period of time (~60 min) could be attributed to the iron particles' slow heat sintering and aggregation during the reaction. This is consistent with the literature[1,3,19] and discussed below.

The impact of different light intensities with the same light source (Hg lamp) on the catalysis was studied (Figure S10), and the results are shown in Figure 1c. Note that no ammonia production was observed until a certain threshold light intensity was achieved, and then the activity clearly increased with light intensity. These results are consistent with the finding that the reverse saturation state of graphene could only be achieved with certain light intensity and the ejected hot electrons (measured as current) increased with light intensity.[28] Importantly, a clear catalytic activity dependence on wavelength was also observed as shown in Figure 1d, where a shorter wavelength, such as Hg lamp (200−600 nm, Figure S11), gave higher activity than Xe (400−780 nm, Figure S12) and tungsten iodine lamps (800−1300 nm, Figure S13) under the same conditions and light power. This echoes the same dependence of the electron

DOI: 10.1021/acsnano.6b06472
ACS Nano 2016, 10, 10507−10515

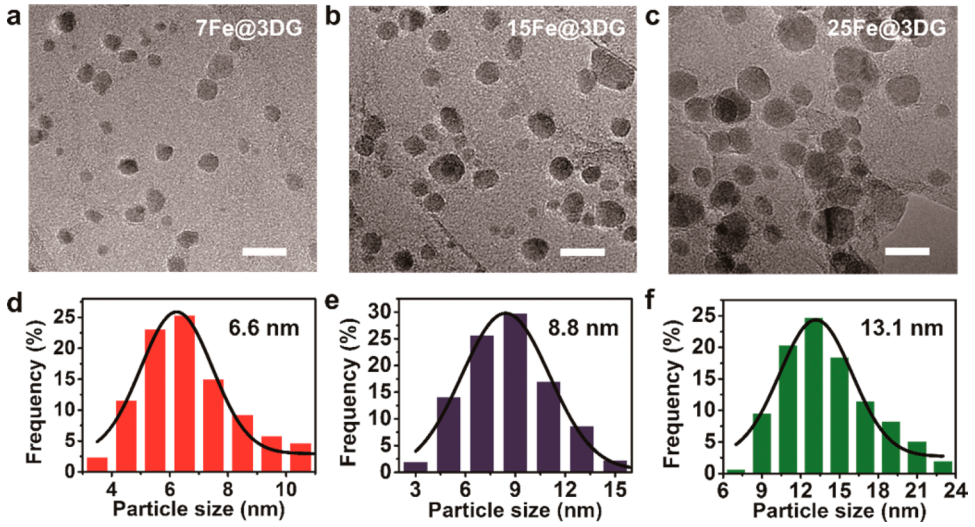

Figure 2. Particle size varies with iron loading. (a–c) TEM images of different iron loading. (d–f) Particle size distributions for a–c, respectively. Scale bars, 20 nm. The histograms are fitted with Gauss distribution.

emission of Fe@3DG materials, as shown in Figure 1e, consistent with the results for the 3DG as reported before.[28]

Importantly, to confirm that all photons from UV to infrared light could activate the reaction, a control experiment was carried out using a Xe lamp as the light source but with a light filter (cut off light below 400 nm completely, Figure S14). The results show that significant activity (~70%) still remained (Figure S15) without photons below 400 nm, indicating that the Fe@3DG catalyst could be activated for ammonia synthesis under a broad wavelength range from ultraviolet to visible to even infrared light.

The apparent activation energy for this light-driven catalysis was measured, as shown in Figure S16. Very notably, under our measured conditions, 7Fe@3DG exhibits an apparent activation energy of 41 kJ mol^{-1}, which is much smaller compared with that of HB catalyst at industry production conditions (~160 kJ mol^{-1}).[33] The much smaller apparent activation energy indicates that both light illumination and graphene play a significant role for the high catalytic activity.

We also found that the catalytic performance of catalysts is related to iron loadings. It has been well accepted that activity of the iron catalyst is dependent on the amount of the actual catalytic sites (active site/center) (C_7, mainly Fe (111) plane)[34] on the nanoscale iron domain in the catalyst. Note that such active sites depend on not only the total iron loading or surface area but also on the size of such Fe domain sizes.[35] This is also reflected in our studies. On the basis of transmission electron microscopy (TEM) analysis (Figure 2) of Fe@3DG with different iron loadings, it has been found that the size of iron oxide particles becomes larger with increased iron loadings. The increased iron loading could reduce specific active site numbers of the catalysts because increased loading will have iron (oxide) domains in larger sizes and wider distribution ranges on the graphene sheets.[36] Thus, as shown in Figures 1a and 2, the optimized catalyst 7Fe@3DG, with an average particle size of 6.6 nm, exhibits the highest catalytic activity.

It is well-known that the lifetime for for iron-based ammonia catalyst is strongly associated with the morphology stability/change of iron domain.[3,19,37] Therefore, the morphology and size distribution before and after the reaction were studied for the lifetime of our catalyst's activity. As shown in Figure 3a,b,

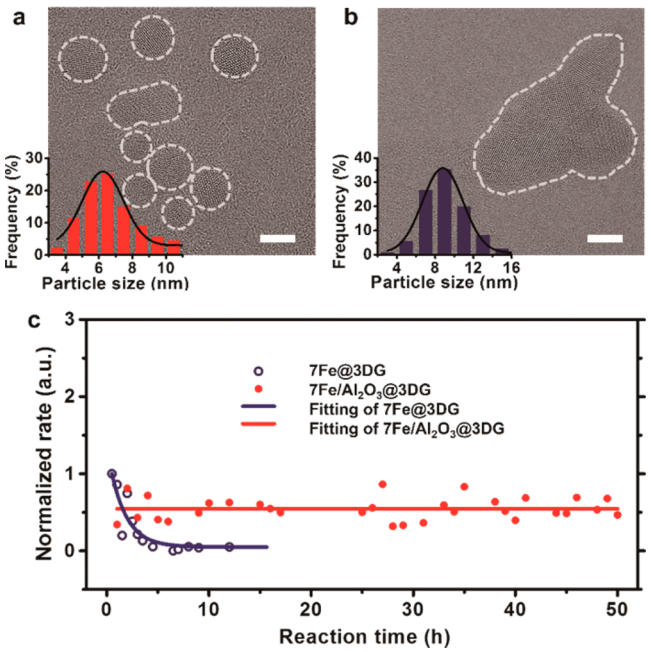

Figure 3. Stability of Fe@3DG catalyst. HR-TEM images of 7Fe@3DG before (a) and after (b) the reaction. The ranges highlighted with white show the catalyst particles. Insets show the corresponding particle size distribution. Scale bars, 4 nm. The histograms are fitted with Gauss distribution. (c) Catalytic activity for ammonia synthesis *vs* time over the structure promoted catalyst 7Fe@3DG and 7Fe/Al_2O_3@3DG. Ammonia synthesis reaction conditions: synthesis gas, H_2/N_2 = 3 (v/v) with a flow rate of 20 mL min^{-1}; pressure, 1 atm; 500 W high-pressure Hg lamp.

degraded activity after a certain period (Figure 1b) was also found for the significantly increased iron domain size caused by iron particle slow heat sintering during the reaction, which is well-known for the Fe and Ru catalysts.[19,37] The long-term stability of HB catalyst is believed to be due to texture promoters such as alumina used in the catalyst. Note that the HB catalyst is actually a ternary oxide with a framework, which works as the structural keeper, thus preventing iron particles from sintering together.[1,3,8] With this knowledge, a similar

DOI: 10.1021/acsnano.6b06472
ACS Nano 2016, 10, 10507–10515

approach was used to improve the stability of our catalyst, where structural promoter Al_2O_3 was loaded together with the iron precursor when the catalyst was prepared (details in the Supporting Information). Indeed, the catalytic activity and stability of the modified catalyst 7Fe/Al_2O_3@3DG retained even during a 50 h test significantly improved compared with that without structural promoter (Figure 3c).

Mechanism. The facts that no detectable or negligible amount of ammonia production from a series of control experiments, including that (1) 7Fe@3DG catalyst was used at the same temperature but without light illumination, (2) only 3DG catalyst (no Fe loading) was used under the same light illumination, and (3) only the same Fe catalyst (no 3DG) was used under the same conditions with the same light illumination (Figure 1a), indicate that not only the atmospheric catalysis is a light-driven result but also the synergetic effect involving both graphene and iron plays an important role.

It has been well documented that the doped alkali metals such as potassium, as the electronic promoter,[1] enhance the catalytic activity significantly in the HB catalyst by increasing the electron density in the vicinity of Fe, thus increasing its π-back-electron donation from Fe d-electrons to the antibonding π^* orbital of N_2. This effect facilitates significantly the activation of N_2 molecule on the Fe surface and thus greatly increases the activity of the catalyst.[8,38,39]

A similar role for the highly energetic hot electrons generated by light from graphene is thus expected for the enhanced or synergetic catalysis for our case.[13,15,18] Note it has been well proven that under light illumination a reverse saturation state of graphene could be achieved with a wide range of light wavelengths up to red with rather low fluence (~4 μJ cm^{-2})[40] including using direct intensive sun light,[28] where a high density of hot (energetic) electrons is achieved. These hot electrons, behaving as massless Dirac fermions, should relax into a hot but thermalized electron distribution equilibrium with significantly high tail energy (well above its Fermi level) under continuous light illumination due to the bottleneck of relaxation at the Dirac point in the band structure near the Fermi level[26] and can be also ejected out from graphene into free space following the LIEE mechanism.[28,41] Thus, we envisage that these hot electrons may have several possible paths to facilitate the activation of N_2 molecules (Figure 4a). In one way, the hot electrons might just work as the electrons from alkali metal[39] or that in the electride (F-center) materials[42,43] to increase the electron density (of the conduction band) at the Fe surface,[15,20] and thus, highly enhanced Fe catalytic activity could be achieved (Figure 4a, path 1a,b). The second possible path (Figure 4a, path 2) might work as a direct electron transfer, where the hot electrons might tunnel through the little Schottky barrier and be accepted by the antibond orbitals of N_2 adsorbed on Fe catalyst.[44] The third possible way (Figure 4a, path 3) is that even the N_2 molecules nearby in the micrometer range around the graphene sheet (but not adsorbed on Fe catalyst as in the case of path 2 above) might be activated directly by accepting these ejected highly energetic electrons[44−46] since the ejected electrons could have energy up to tens of eV[28] and can traverse in the range of over 100 nm.[47,48] The exact contribution from each of these possible paths or if there is any other path is yet to be understood. Also, transfer of these hot electrons to the acceptors (orbitals) should be very complicated, and investigation is still underway.[47,49] It is expected that, in similar ways, the hot electrons are anticipated

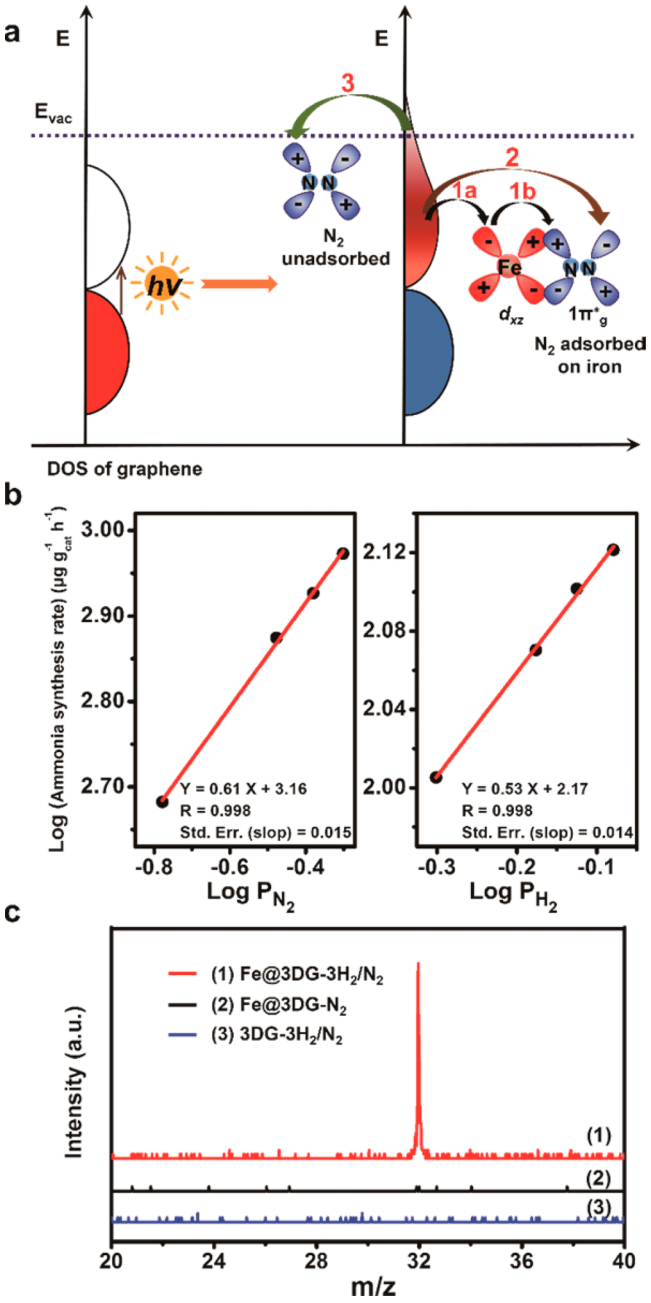

Figure 4. Activation mechanism over Fe@3DG under light illumination. (a) Three possible paths of the hot electrons generated from light illuminated graphene to prompt the activation of N_2 molecule (arrows labeled with 1a,b, 2, and 3). Left: electronic density of states (DOS) for graphene's valence band before light illumination. (b) Reaction orders of N_2 and H_2 for ammonia synthesis using 7Fe@3DG catalyst. (c) Mass spectra results using API-TOFMS.

to increase the rate of H_2 dissociation,[44,50] thus prompting the overall reaction.

The enhanced catalytic performance by hot electrons also impacts the reaction orders significantly, as shown in Figure 4b. Note that the measured reaction order for N_2 is 0.61, indicating that the N_2 dissociation is much more efficient than the conventional Fe/Ru-based catalysts, where the order is generally a unit.[20,51] The reaction order for H_2 is measured at 0.53, also significantly lower than the conventionally fused Fe catalyst (~2.0),[51] which can also be attributed to the enhanced

DOI: 10.1021/acsnano.6b06472
ACS Nano 2016, 10, 10507−10515

efficient dissociation of H_2 due to the same hot electron effect.[10]

One of the best ways to understand any mechanism would be to observe or best isolate (catch) the intermediates. For the case of ammonia synthesis, while there are still lots of puzzles, it has been proposed that intermediates such as various N_xH_y could exist.[52] Indeed, when a noncommercial atmospheric pressure ionization time-of-flight mass spectrometer (API-TOFMS) was used (for details, see the Supporting Information and Figure S17), an intermediate N_2H_4 was detected (Figure 4c), similar to the case for the photoactivated TiO_2 catalysis.[18] Note that no N_2H_4 was detected in the final product (details in the Supporting Information).

With these results in hand, though the precise mechanism is still not clear, we envisage that the general reaction mechanism (Figure 5) in our case would be where the important N−N

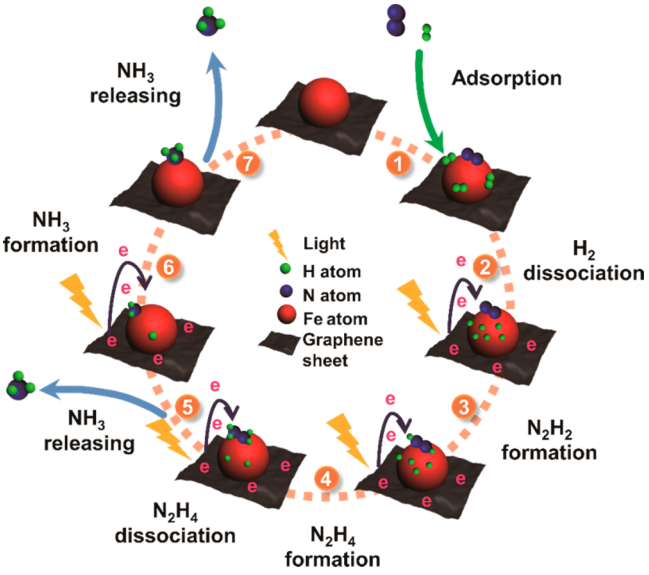

Figure 5. Proposed pathway for the ammonia synthesis using Fe@3DG catalyst under light illumination.

bond breakage probably happens at a late stage. Thus, the addition of predissociated H atom to molecular N_2 happens first to form intermediate N_2H_2 and N_2H_4[18,21] before the N−N bond breakage.[24,25,53−56]

CONCLUSIONS

It is important to note this ammonia catalytic system combines several important advantages including that driven only by light from N_2 and H_2 molecules directly and operated under atmospheric pressure and milder temperature without external heating. Also, no external voltage or electrochemical process or sacrificial agent is required. Due to its zero bandgap structure of graphene and essentially wavelength-independent but efficient absorption, this catalysis system can work with all visible light up to red. In this aspect, it is superior to other conventional semiconductors such as TiO_2,[18] diamond,[21,43] and GaP[13] where the limitation of their bandgap allows them to utilize light mostly in the ultraviolet range. Our results also demonstrate a mechanism for photocatalysis using hot electrons, generated from graphene, with high reducing power for reactions which are otherwise unachievable using conventional approaches.

There should be ample room to advance this pathway if combined with many of the current sophisticated catalysis technologies. First, the production rate is very likely to become orders higher if high pressure similar to that for HB catalyst is applied following the Le Chatelier's principle. In addition, a hybrid approach combining this light-induced catalysis with the current state-of-the-art HB process might be expected for a more efficient production of ammonia under milder conditions with significant energy cost advantage. Overall, the use of graphene, prepared easily on a large scale from graphite directly, suggests it might work as an efficient electron reservoir and represent a paradigm for a cost-efficient yet powerful photocatalytic reduction system with only visible (sun) light as the energy source. While the rather multidisciplinary hot-electron generation and applications are still in their very early infancy, including exact energy transfer, relaxing, and transportation mechanisms, these findings based on the two-dimensional and easily accessible graphene material are expected to open up some room for both fundamental studies and industry applications. Similar studies are also expected to be prompted for other two-dimensional materials with Dirac-like band structures.

EXPERIMENTAL SECTION

Synthesis of 3DGraphene (3DG) and Fe@3DGraphene (Fe@3DG). The starting material, graphene oxide (GO), was synthesized by the oxidation of natural graphite powder using a modified Hummers' method based on references published elsewhere.[57,58] Three-dimensional graphene, denoted as 3DGraphene (3DG), was prepared following our previous procedures.[27,28] A GO ethanol solution (70 mL, 0.375 mg mL^{-1}) was sealed in a 100 mL Teflon-lined autoclave, heated to 180 °C, and maintained at this temperature for 12 h. The autoclave was then naturally cooled to room temperature. Then the as-prepared ethanol-filled intermediate product was carefully removed from the autoclave to have a slow and gradually solvent exchange with water. After the solvent-exchange process was totally completed, the water-filled product was freeze-dried and then dried in a vacuum oven at 120 °C for 12 h. Finally, the sample was annealed at 450 °C for 6 h in H_2/Ar mixture gas (5/95, v/v) to obtain the final graphene material (3DG). 3DGraphene loaded with different weight of iron oxide (denoted as Fe@3DG) were synthesized through the similar process as described above using $Fe(NO_3)_3{\cdot}9H_2O$ (98%, J&K Technology Co., Ltd.) as the iron precursor in the GO dispersion. As a typical example, for the catalyst 7Fe@3DG, an ethanol solution of $Fe(NO_3)_3{\cdot}9H_2O$ (34 mL, 0.37 mg mL^{-1}) and a GO ethanol dispersion (36 mL, 0.73 mg mL^{-1}) were mixed and then stirred for 2 h. The solution was then treated as the same solvothermal process of 3DG described above. The as-prepared ethanol-filled intermediate product was slow and gradually solvent exchanged with water and then freeze-dried. The final product was obtained by the same annealing as above. The final Fe loading was measured at 6.9 wt % using atomic emission spectrometry with inductively coupled plasma (ICP-AES) (details in the Supporting Information), thus denoted as 7Fe@3DG for convenience. Similarly, a series of Fe@3DG materials were synthesized (with iron loading of ~2, 15, 25, and 50 wt %) and designated as 2Fe@3DG, 15Fe@3DG, 25Fe@3DG,, and 50Fe@3DG, respectively. The details of exactly measured iron loading and naming of the products are shown in Table S1. The mean size of iron oxide in 2Fe@3DG, 7Fe@3DG 15Fe@3DG, 25Fe@3DG, and 50Fe@3DG was estimated with a measured diameter from a minimum of 100 particles in TEM images for each sample and was 3.2, 6.6, 8.8, 13.1, and 15.1 nm, respectively. A series of control catalysts, including 7Fe, 7Fe@AC, 7BulkFe@3DG, HB Fe, and 7Fe/Al_2O_3@3DG, were synthesized through a similar process as described above and detailed in the Supporting Information.

Ammonia Synthesis. Reactions were carried out in a homemade glass fixed-bed continuous-flow reactor with an inside diameter of 34 mm and a height of 260 mm. As shown in Figure S5, the catalyst, high-pressure Hg lamp (500 W, Shanghai Jiguang Special Lighting Electrical

DOI: 10.1021/acsnano.6b06472
ACS Nano 2016, 10, 10507−10515

Appliance Factory), and temperature probe were placed together in the center of the reactor, which was also surrounded by a water cooling jacket, and sealed. The synthesis gas (high purity, 99.999%) of H_2/N_2 (3/1, v/v) was flowed through the catalyst bed with a rate of 20 mL min^{-1}. The reaction was carried out at atmospheric pressure, and the catalyst temperature was ~200 (±10) °C due to the light heating. The gas-phase effluent was passed into a customized absorption bottle, which contains the diluted H_2SO_4 (60.00 mL, 0.0025 mol L^{-1}), to capture the ammonia produced, and then this absorption solution was analyzed by the indophenol blue method (details in Ammonia Measurement Methods). The ammonia production amounts over various catalysts including 2Fe@3DG (240 mg), 7Fe@3DG (240 mg), 15Fe@3DG (300 mg), 25Fe@3DG (850 mg), 50Fe@3DG (850 mg), 7Fe@AC (18.0 g), 7BulkFe@3DG (230 mg), HB Fe (20.0 g), 7Fe (8.5 g), and 3DG (177 mg) are shown in Figure 1a. Note that in order to keep the constant catalyst volume at roughly same cross area for light absorption, the weights are different. Other catalysis reactions with different conditions, such as, heating without light illumination, catalytic reactions with different light intensity, catalytic reactions using different light sources (wavelength), and catalytic lifetime test, are detailed in the Supporting Information.

Note that possible contamination such as that from the reactive N_2/H_2 should be excluded on the basis of the following control experiments. In addition to the high purity (99.999%) of N_2/H_2 used in the experiments, more importantly, in Figure 1a, no NH_3 was detected in the experiments of 3DG catalyst in the same $3H_2/N_2$ and Fe@3DG catalyst in the same $3H_2/N_2$ induced only by heat, showing no NH_3 contamination existed in the N_2/H_2 source.

Ammonia Measurement Methods. (a) The Indophenol Blue Method. This follows the literature.[21] A 2.00 mL absorption solution taken from the absorption bottle was transferred to a colorimetric tube and diluted to 10.00 mL with water. Then an aqueous solution of $Na[Fe(NO)(CN)_5]$ (100 μL, 1 wt %, Sigma-Aldrich), salicylic acid solution (500 μL, 5 wt %, Sigma-Aldrich) and NaClO aqueous solution (100 μL, 0.05 M, Tianjin Heowns Biochemical Technology Co., Ltd.) were in turn added to the absorption solution and homogeneously mixed. After 1 h of standing at room temperature, the absorption spectrum was carried out using a JASCO V-570 UV−vis spectrophotometer. The formation of indophenol blue was determined using the absorbance at the wavelength of 704 nm. Absolute calibration of the method was achieved using standard ammonium chloride solutions, prepared from the standard solid ammonium chloride (99.99%, Sigma-Aldrich). **(b) Online Real-Time Mass Spectrometry Analysis.** This real-time and online analysis method was based on our co-worker's earlier reported work,[32] which was used to study the kinetics and thermodynamics of the catalytic reactions (details in the Supporting Information), including (1) activity *vs* time (Figure 1b), (2) activity *vs* light intensity (Figure 1c), (3) activity *vs* light sources with different wavelength (Figure 1d), (4) apparent activation energy (Figure S16), and (5) reaction orders (Figure 4b). A vacuum ultraviolet (VUV) lamp-based (10.6 eV, Cathodeon Ltd., Cambridge, U.K.) charge-transfer ionization ion source with O_2^+ as the reagent ions in a home-built orthogonal acceleration time-of-flight mass spectrometer (charge-transfer ionization time-of-flight mass spectrometry, CTI-TOFMS) has been applied for real-time monitoring of the ammonia synthesis in a reactor. The CTI ion source with a pressure of about 40 Pa was separated into two regions: a reagent ion-producing region and ion−molecule reaction region. Briefly, the effluent gas from the ammonia synthesis reactor and the reagent gas O_2 were directly introduced into the reagent ion-producing region and the ion−molecule reaction region through a 250 μm i.d., 0.5 m long deactivated fused-silica capillary and a 200 μm i.d., 0.5 m long deactivated fused-silica capillary, respectively. For the necessity of long-term stable monitoring, a self-adjustment algorithm for stabilizing O_2^+ ion intensity was developed to automatically compensate the attenuation of the O_2^+ ion yield in the ion source as a result of the oxidation of the photoelectric electrode and contamination on the MgF_2 window of the VUV lamp. As a result, the limit of quantification for ammonia was in ppbv (parts per billion by volume) when the signal intensity of O_2^+ reagent ions was stabilized at 300000 counts, which is adequate for online analysis of NH_3 in microcatalytic reactions. The TOF mass analyzer was operated in linear mode with a mass resolution of 900 (fwhm) at m/z = 78. Each data point was accumulated in real time for 30 s by a 100 ps time-to-digital converter (TDC) (model 9353, Ametek, Inc., Oak Ridge, TN) at a repetition rate of 33 kHz. The qualitative analysis results of ammonia are shown in Figure S8. The signal at m/z = 17 is assigned to NH_3^+, and the signal at m/z = 18 indicates the produced H_2O^+ or NH_4^+. Note that OH^+ could not be produced because the recombination energy of O_2^+ (12.07 eV)[32] is lower than the ionization energy of H_2O to H and OH (16.95 eV),[59] and the charge transfer from O_2^+ to OH (from H_2O) is invalid. Hydrazine measurement is discussed in the Supporting Information.

Hot Electron Emission with Different Light Wavelength and Intensity. The detection of electrons from Fe@3DG illuminated by laser with different wavelengths and intensity was conducted as described in our previously reported work.[28] As detailed, a Fe@3DG sample (0.7 × 0.7 × 0.5 cm^3) was placed inside a metal box (as the electron-collecting electrode), which was positioned in a high vacuum (6.7×10^{-6} Torr) chamber with a quartz window, and a laser (spot area, ~ 4 mm^2) illuminated sample through the quartz window. The current signal was recorded by a digital oscilloscope (Rigol DS1102E, 1 GSa s^{-1}, 100 MHz). Note that the laser sources are all continuous lasers, and the powers (and the power densities) are thus all average powers (and average power densities), not like that of the peak power when pulse laser sources are used in many cases. The laser source devices used here were purchased from Shaanxi Alaxy Technologies Photonics Co., and these included models of PT-LD-650-3W-FCL, PT-DPL-532-3W-FCL, and PT-DPL-450-3W-FCL, which were calibrated using laser power/energy meters/sensors (Ophir Nova II and 10A-P). The wavelength of the laser with 450, 532, and 650 nm was selected, and the intensity of every wavelength was set at 2.43, 2.55, 2.68, 2.85, and 3.00 W, respectively. The mathematical calculation of the average current signal intensity was performed as reported previously.[28] The results are shown in Figure 1c.

ASSOCIATED CONTENT

Supporting Information

The Supporting Information is available free of charge on the ACS Publications website at DOI: 10.1021/acsnano.6b06472.

Detailed experimental procedures, including the synthesis of a series of catalysts, catalysis experiments, intermediate detection method, thermodynamic and kinetic studies, and other supplementary figures (PDF)

AUTHOR INFORMATION

Corresponding Author

*E-mail: yschen99@nankai.edu.cn.

Author Contributions

‖Y.L., Y.Y., and T.Z. contributed equally to this work.

Notes

The authors declare no competing financial interest.

ACKNOWLEDGMENTS

We gratefully acknowledge financial support from the Ministry of Science and Technology of China (MoST, 2016YFA0200200), the National Natural Science Foundation of China (NSFC, 51633002, 51472124, 51273093, and 51502125), and the Natural Science Foundation of Hebei Province of China (E2016408035). We thank Yuting Shen and Litao Sun (Southeast University) for help with HR-TEM measurements and Jingyin Xu and Qiang Wang (Lanzhou University) for kinetics measurements.

DOI: 10.1021/acsnano.6b06472
ACS Nano 2016, 10, 10507−10515

REFERENCES

(1) Ertl, G. Reactions at Surfaces: From Atoms to Complexity (Nobel Lecture). *Angew. Chem., Int. Ed.* **2008**, *47*, 3524−3535.
(2) Galloway, J. N.; Townsend, A. R.; Erisman, J. W.; Bekunda, M.; Cai, Z.; Freney, J. R.; Martinelli, L. A.; Seitzinger, S. P.; Sutton, M. A. Transformation of the Nitrogen Cycle: Recent Trends, Questions, and Potential Solutions. *Science* **2008**, *320*, 889−892.
(3) Kandemir, T.; Schuster, M. E.; Senyshyn, A.; Behrens, M.; Schlögl, R. The Haber-Bosch Process Revisited: On the Real Structure and Stability of "Ammonia Iron" under Working Conditions. *Angew. Chem., Int. Ed.* **2013**, *52*, 12723−12726.
(4) Jia, H. P.; Quadrelli, E. A. Mechanistic Aspects of Dinitrogen Cleavage and Hydrogenation to Produce Ammonia in Catalysis and Organometallic Chemistry: Relevance of Metal Hydride Bonds and Dihydrogen. *Chem. Soc. Rev.* **2014**, *43*, 547−564.
(5) Liu, H. Z. Ammonia Synthesis Catalyst 100 Years: Practice, Enlightenment and Challenge. *Chin. J. Catal.* **2014**, *35*, 1619−1640.
(6) Schlögl, R. Catalytic Synthesis of Ammonia-a "Never-Ending Story"? *Angew. Chem., Int. Ed.* **2003**, *42*, 2004−2008.
(7) Macleod, K. C.; Holland, P. L. Recent Developments in the Homogeneous Reduction of Dinitrogen by Molybdenum and Iron. *Nat. Chem.* **2013**, *5*, 559−565.
(8) Ertl, G. Elementary Steps in Heterogeneous Catalysis. *Angew. Chem., Int. Ed. Engl.* **1990**, *29*, 1219−1227.
(9) Honkala, K.; Hellman, A.; Remediakis, I. N.; Logadottir, A.; Carlsson, A.; Dahl, S.; Christensen, C. H.; Nørskov, J. K. Ammonia Synthesis from First-Principles Calculations. *Science* **2005**, *307*, 555−558.
(10) Kitano, M.; Kanbara, S.; inoue, Y.; Kuganathan, N.; Sushko, P. V.; Yokoyama, T.; Hara, M.; Hosono, H. Electride Support Boosts Nitrogen Dissociation over Ruthenium Catalyst and Shifts the Bottleneck in Ammonia Synthesis. *Nat. Commun.* **2015**, *6*, 6731.
(11) Marnellos, G.; Stoukides, M. Ammonia Synthesis at Atmospheric Pressure. *Science* **1998**, *282*, 98−100.
(12) Murakami, T.; Nishikiori, T.; Nohira, T.; Ito, Y. Electrolytic Synthesis of Ammonia in Molten Salts under Atmospheric Pressure. *J. Am. Chem. Soc.* **2003**, *125*, 334−335.
(13) Dickson, C. R.; Nozik, A. J. Nitrogen Fixation *via* Photo-enhanced Reduction on P-Gallium Phosphide Electrodes. *J. Am. Chem. Soc.* **1978**, *100*, 8007−8009.
(14) Lan, R.; Irvine, J. T.; Tao, S. Synthesis of Ammonia Directly from Air and Water at Ambient Temperature and Pressure. *Sci. Rep.* **2013**, *3*, 1145.
(15) Oshikiri, T.; Ueno, K.; Misawa, H. Plasmon-induced Ammonia Synthesis through Nitrogen Photofixation with Visible Light Irradiation. *Angew. Chem., Int. Ed.* **2014**, *53*, 9802−9805.
(16) Lan, R.; Tao, S. W. Electrochemical Synthesis of Ammonia Directly from Air and Water Using a $Li^+/H^+/NH_4^+$ Mixed Conducting Electrolyte. *RSC Adv.* **2013**, *3*, 18016−18021.
(17) Yamauchi, M.; Abe, R.; Tsukuda, T.; Kato, K.; Takata, M. Highly Selective Ammonia Synthesis from Nitrate with Photocatalytically Generated Hydrogen on $CuPd/TiO_2$. *J. Am. Chem. Soc.* **2011**, *133*, 1150−1152.
(18) Schrauzer, G. N.; Guth, T. D. Photocatalytic Reactions. Photolysis of Water and Photoreduction of Nitrogen on Titanium Dioxide. *J. Am. Chem. Soc.* **1977**, *99*, 7189−7193.
(19) Licht, S.; Cui, B.; Wang, B.; Li, F. F.; Lau, J.; Liu, S. Ammonia Synthesis. Ammonia Synthesis by N_2 and Steam Electrolysis in Molten Hydroxide Suspensions of Nanoscale Fe_2O_3. *Science* **2014**, *345*, 637−640.
(20) Kitano, M.; inoue, Y.; Yamazaki, Y.; Hayashi, F.; Kanbara, S.; Matsuishi, S.; Yokoyama, T.; Kim, S. W.; Hara, M.; Hosono, H. Ammonia Synthesis Using a Stable Electride as an Electron Donor and Reversible Hydrogen Store. *Nat. Chem.* **2012**, *4*, 934−940.
(21) Zhu, D.; Zhang, L. H.; Ruther, R. E.; Hamers, R. J. Photo-Illuminated Diamond as A Solid-State Source of Solvated Electrons in Water for Nitrogen Reduction. *Nat. Mater.* **2013**, *12*, 836−841.
(22) Brown, K. A.; Harris, D. F.; Wilker, M. B.; Rasmussen, A.; Khadka, N.; Hamby, H.; Keable, S.; Dukovic, G.; Peters, J. W.; Seefeldt, L. C. Light-driven Dinitrogen Reduction Catalyzed by a CdS:Nitrogenase MoFe Protein. *Science* **2016**, *352*, 448−450.
(23) Van der Ham, C. J.; Koper, M. T.; Hetterscheid, D. G. Challenges in Reduction of Dinitrogen by Proton and Electron Transfer. *Chem. Soc. Rev.* **2014**, *43*, 5183−5191.
(24) Hoffman, B. M.; Lukoyanov, D.; Dean, D. R.; Seefeldt, L. C. Nitrogenase: A Draft Mechanism. *Acc. Chem. Res.* **2013**, *46*, 587−595.
(25) Hoffman, B. M.; Dean, D. R.; Seefeldt, L. C. Climbing Nitrogenase: Toward a Mechanism of Enzymatic Nitrogen Fixation. *Acc. Chem. Res.* **2009**, *42*, 609−619.
(26) Brida, D.; Tomadin, A.; Manzoni, C.; Kim, Y. J.; Lombardo, A.; Milana, S.; Nair, R. R.; Novoselov, K. S.; Ferrari, A. C.; Cerullo, G.; et al. Ultrafast Collinear Scattering and Carrier Multiplication in Graphene. *Nat. Commun.* **2013**, *4*, 1987.
(27) Wu, Y. P.; Yi, N. B.; Huang, L.; Zhang, T. F.; Fang, S. L.; Chang, H. C.; Li, N.; Oh, J.; Lee, J. A.; Kozlov, M.; et al. Three-Dimensionally Bonded Spongy Graphene Material with Super Compressive Elasticity and Near-Zero Poisson's Ratio. *Nat. Commun.* **2015**, *6*, 6141.
(28) Zhang, T. F.; Chang, H. C.; Wu, Y. P.; Xiao, P. S.; Yi, N. B.; Lu, Y. H.; Ma, Y. F.; Huang, Y.; Zhao, K.; Yan, X. Q.; et al. Macroscopic and Direct Light Propulsion of Bulk Graphene Material. *Nat. Photonics* **2015**, *9*, 471−476.
(29) Tielrooij, K. J.; Song, J. C. W.; Jensen, S. A.; Centeno, A.; Pesquera, A.; Zurutuza Elorza, A.; Bonn, M.; Levitov, L. S.; Koppens, F. H. L. Photoexcitation Cascade and Multiple Hot-Carrier Generation in Graphene. *Nat. Phys.* **2013**, *9*, 248−252.
(30) Zhang, L.; Zhu, D.; Nathanson, G. M.; Hamers, R. J. Selective Photoelectrochemical Reduction of Aqueous CO_2 to CO by Solvated Electrons. *Angew. Chem., Int. Ed.* **2014**, *53*, 9746−9750.
(31) Matsuishi, S.; Toda, Y.; Miyakawa, M.; Hayashi, K.; Kamiya, T.; Hirano, M.; Tanaka, I.; Hosono, H. High-Density Electron Anions in a Nanoporous Single Crystal: $[Ca_{24}Al_{28}O_{64}]^{4+}(4e^-)$. *Science* **2003**, *301*, 626−629.
(32) Xie, Y.; Hua, L.; Hou, K.; Chen, P.; Zhao, W.; Chen, W.; Ju, B.; Li, H. Long-Term Real-Time Monitoring Catalytic Synthesis of Ammonia in a Microreactor by VUV-Lamp-Based Charge-Transfer Ionization Time-of-Flight Mass Spectrometry. *Anal. Chem.* **2014**, *86*, 7681−7687.
(33) Liu, H.*Ammonia Synthesis Catalysts: Innovation and Practice*; Chemical Industry Press: Beijing, 2013; pp 41.
(34) Strongin, D. The Importance of C_7 Sites and Surface Roughness in the Ammonia Synthesis Reaction over Iron. *J. Catal.* **1987**, *103*, 213−215.
(35) Fernández, C.; Sassoye, C.; Debecker, D. P.; Sanchez, C.; Ruiz, P. Effect of the Size and Distribution of Supported Ru Nanoparticles on Their Activity in Ammonia Synthesis under Mild Reaction Conditions. *Appl. Catal., A* **2014**, *474*, 194−202.
(36) Arabczyk, W.; Jasińska, I.; Pelka, R. Measurements of the Relative Number of Active Sites on Iron Catalyst for Ammonia Synthesis by Hydrogen Desorption. *Catal. Today* **2011**, *169*, 97−101.
(37) Guo, X.; Fang, G.; Li, G.; Ma, H.; Fan, H.; Yu, L.; Ma, C.; Wu, X.; Deng, D.; Wei, M.; et al. Direct, Nonoxidative Conversion of Methane to Ethylene, Aromatics, and Hydrogen. *Science* **2014**, *344*, 616−619.
(38) Dahl, S.; Logadottir, A.; Jacobsen, C. J. H.; Nørskov, J. K. Electronic Factors in Catalysis: The Volcano Curve and the Effect of Promotion in Catalytic Ammonia Synthesis. *Appl. Catal., A* **2001**, *222*, 19−29.
(39) Ertl, G.; Weiss, M.; Lee, S. B. The Role of Potassium in the Catalytic Synthesis of Ammonia. *Chem. Phys. Lett.* **2013**, *589*, 18−20.
(40) Jensen, S. A.; Mics, Z.; Ivanov, I.; Varol, H. S.; Turchinovich, D.; Koppens, F. H.; Bonn, M.; Tielrooij, K. J. Competing Ultrafast Energy Relaxation Pathways in Photoexcited Graphene. *Nano Lett.* **2014**, *14*, 5839−5845.
(41) Winzer, T.; Knorr, A.; Malic, E. Carrier Multiplication in Graphene. *Nano Lett.* **2010**, *10*, 4839−4843.
(42) Kim, S. W.; Shimoyama, T.; Hosono, H. Solvated Electrons in High-Temperature Melts and Glasses of the Room-Temperature Stable Electride $[Ca_{24}Al_{28}O_{64}]^{4+}(4e^-)$. *Science* **2011**, *333*, 71−74.

DOI: 10.1021/acsnano.6b06472
ACS Nano 2016, 10, 10507−10515

(43) Nebel, C. E. Photocatalysis: A Source of Energetic Electrons. *Nat. Mater.* **2013**, *12*, 780−781.
(44) Mukherjee, S.; Libisch, F.; Large, N.; Neumann, O.; Brown, L. V.; Cheng, J.; Lassiter, J. B.; Carter, E. A.; Nordlander, P.; Halas, N. J. Hot Electrons Do the Impossible: Plasmon-Induced Dissociation of H_2 on Au. *Nano Lett.* **2013**, *13*, 240−247.
(45) Bonn, M.; Funk, S.; Hess, C.; Denzler, D. N.; Stampfl, C.; Scheffler, M.; Wolf, M.; Ertl, G. Phonon- *Versus* Electron-Mediated Desorption and Oxidation of CO on Ru(0001). *Science* **1999**, *285*, 1042−1045.
(46) Knight, M. W.; Sobhani, H.; Nordlander, P.; Halas, N. J. Photodetection with Active Optical Antennas. *Science* **2011**, *332*, 702−704.
(47) Schwede, J. W.; Sarmiento, T.; Narasimhan, V. K.; Rosenthal, S. J.; Riley, D. C.; Schmitt, F.; Bargatin, I.; Sahasrabuddhe, K.; Howe, R. T.; Harris, J. S.; et al. Photon-Enhanced Thermionic Emission from Heterostructures with Low Interface Recombination. *Nat. Commun.* **2013**, *4*, 1576.
(48) Lundstrom, M.*Fundamentals of Carrier Transport*; Cambridge University Press: Cambridge, 2011; pp 357−359.
(49) Wu, K.; Chen, J.; McBride, J. R.; Lian, T. Efficient Hot-Electron Transfer by a Plasmon-Induced Interfacial Charge-Transfer Transition. *Science* **2015**, *349*, 632−635.
(50) Sil, D.; Gilroy, K. D.; Niaux, A.; Boulesbaa, A.; Neretina, S.; Borguet, E. Seeing Is Believing: Hot Electron Based Gold Nanoplasmonic Optical Hydrogen Sensor. *ACS Nano* **2014**, *8*, 7755−7762.
(51) Hagen, S. Ammonia Synthesis with Barium-Promoted Iron−Cobalt Alloys Supported on Carbon. *J. Catal.* **2003**, *214*, 327−335.
(52) Hwang, D. Y.; Mebel, A. M. Reaction Mechanism of N_2/H_2 Conversion to NH_3: A Theoretical Study. *J. Phys. Chem. A* **2003**, *107*, 2865−2874.
(53) Rod, T. H.; Nørskov, J. K. Modeling the Nitrogenase FeMo Cofactor. *J. Am. Chem. Soc.* **2000**, *122*, 12751−12763.
(54) Hinnemann, B.; Nørskov, J. K. Chemical Activity of the Nitrogenase FeMo Cofactor with a Central Nitrogen Ligand: Density Functional Study. *J. Am. Chem. Soc.* **2004**, *126*, 3920−3927.
(55) Le, Y. Q.; Gu, J.; Tian, W. Q. Nitrogen-Fixation Catalyst Based on Graphene: Every Part Counts. *Chem. Commun.* **2014**, *50*, 13319−13322.
(56) Schrock, R. R. Catalytic Reduction of Dinitrogen to Ammonia by Molybdenum: Theory *Versus* Experiment. *Angew. Chem., Int. Ed.* **2008**, *47*, 5512−5522.
(57) Becerril, H. A.; Mao, J.; Liu, Z.; Stoltenberg, R. M.; Bao, Z.; Chen, Y. Evaluation of Solution-Processed Reduced Graphene Oxide Films as Transparent Conductors. *ACS Nano* **2008**, *2*, 463−470.
(58) Zhang, L.; Liang, J.; Huang, Y.; Ma, Y.; Wang, Y.; Chen, Y. Size-Controlled Synthesis of Graphene Oxide Sheets on a Large Scale Using Chemical Exfoliation. *Carbon* **2009**, *47*, 3365−3368.
(59) NIST National institute of Standards and Technology (NIST). http://webbook.nist.gov/chemistry/ (accessed Sep 26, 2016).

DOI: 10.1021/acsnano.6b06472
ACS Nano 2016, 10, 10507−10515